(RESEARCH ARTICLE)

Check for updates

Comparative study of the thermal performances of a solar tower

Moctar Ousmane [1, 3, *], Thierry Sikoudouin Maurice KY [3], B. Magloire Pakouzou [3, 5], Amadou konfé [3], Germain Wende Pouiré Ouedraogo [3, 4], Salifou Ouédraogo [3], Boureima Kaboré [2, 3], Dianda Boureima [3, 6], KAM Sié [3] and Dieudonné Joseph Bathiébo [3]

[1] University of Agadez, PO BOX 199, Niger.
[2] Département de Physique, UFR-ST, Université Norbert ZONGO, Burkina Faso.
[3] Laboratory L.E.T.R.E, Université Joseph KI-ZERBO, Burkina Faso.
[4] ESI, Université de Fada N'Gourma, Burkina Faso.
[5] Université de Bangui, R.C. A.
[6] Institut de Recherche en Sciences Appliquées et Technologies, Burkina Faso.

Abstract

This work presents a comparative experimental study of the thermal performances of two types of solar chimneys. The objective is to compare the thermal performances of a solar chimney with a hyperbolic collector associated to a plane absorber painted black. We used a second collector a collectors equipped with hemispherical concentrators. To do this, we designed an experimental device at the central maintenance workshop of Ouagadougou 's University. Measurements carried out on the device with the hot wire anemometer, a data logger and a pyranometer allowed us to conclude that the device with hyperbolic collectors associated with hemispherical concentrators is more advantageous than that with a plane absorber in terms of thermal performance. From these results, we show that the temperature and speed of the air change depending on the amount of sunshine.

Keywords: Solar chimney; Hyperbolic collector; Hemispherical concentrator; Experimental study.

1. Introduction

In solar energy, we distinguish two types of solar collectors: non-concentrating or stationary solar collectors and concentrating solar collectors. Let us specify that for the planar or stationary solar collector the surface of this collector and the surface of absorption of solar radiation are identical. However, concentrated solar collectors have a sun tracking system and are equipped with concave reflective surfaces capable of intercepting and concentrating solar radiation on a reduced surface area, thus increasing the solar flux [1]. Note that these concentrating solar collectors are equipped with either one axis or two axes for tracking the sun as indicated in table 1 [2]. We can also classify stationary solar collectors according to the temperature level: low temperature, medium temperature, high temperature collectors. Following this classification, we distinguish three types of solar thermal collectors which are: the flat collector, the vacuum tube collector, and the concentration collector [3]. Cisse et al. [4] experimented a solar chimney's collector equipped with a concentration system. They obtained a rise in temperature leading to a speed increase compared to a conventional collector without a concentration system. Chaichan et al. [5] studied the impact of dust and pollution deposits on the performance of a solar chimney. They found that the closer the cleaning periods, the higher the efficiency of the solar chimney. Ahmed et al. [6] experimented with two models of solar chimney A and B. System (A) had a glass collector and a photovoltaic panel as absorber with a chimney of 2 m height while system (B) is like system (A) but with a photovoltaic panel as collector and plywood as absorber. They concluded that the power produced by system (B) is greater than the power produced by system (A). To reduce heat loss by convection and radiation, transparent insulation

* Corresponding author: Moctar Ousmane

was used like Teflon materials. Despite the mechanical deflection disadvantage of Teflon, flat sensors fitted with Teflon overcame this problem and showed their ability to operate up to 120°C with good performance [7]. Platzer et al. [8] developed and tested several prototypes of planar sensors with transparent honeycomb insulating materials. These studies demonstrated that convective heat losses are significantly reduced using transparent insulation materials. To compensate for the overheating of these flat sensors, Harrison et al. [9] used a ventilation channel to limit the temperature of these planar sensors in climates where there is a potential risk of freezing temperatures and to prevent corrosion of system components. Kessentini et al. [10] experimented a flat sensor with transparent plastic insulation equipped with a low-cost overheating protection system. They concluded on the effectiveness of the overheating system capable of maintaining sufficiently low temperatures at the level of the flat sensor, thus preventing the degradation of the transparent insulating materials. Mandal et al. [11] studied the impact of chimney configuration and collector inclination on the energy efficiency of a chimney solar power plant. They proved that chimneys with abrupt divergence or inclined collectors are beneficial for improving the performance of a solar chimney. In addition, they showed that the combination of an inclined collector (γ=0.6°) and a divergent chimney ($\emptyset$=0.75°) improves the power by 80% or 92kW. Li et al. [12] experimented the efficiency of a solar chimney plant with a phase change material under three different fluxes: $600 W/m^2$, $500 W/m^2$ and $700 W/m^2$. The results showed that even if at $600\ W/m2$ and $500\ W/m2$ the phase change material does not melt completely, the temperature of the absorber changes because the three heat fluxes for the same charging period of 7 h 10 min are the same during the phase change transition period. Unlike discharging during the thermally sensitive period, surface temperatures drop relatively slowly throughout the phase shift period until the latent heat is completely released. For all the examples studied, the phase change periods are approximately 13 h 50 min. Air flow rates change depending on the absorber temperature. The airflow for $700\ W/m^2$ is 0.04 kg/s, which is slightly higher than the 0.039 kg/s for $600\ W/m^2$ and 0.038 kg/s for 500 W/m².

After this reminder on solar collectors and absorbers, we will present you a comparative study of the two solar chimneys thermal performances.

Table 1 Solar energy collectors

Motion	Collector type	Absorber type	Concentration ratio	Indicative temperature range (°C)
Stationary	Flat plate collector (FPC)	Flat	1	30-80
	Evacuated tube collector (ETC)	Flat	1	50-200
	Compound parabolic collector (CPC)	Tubular	1-5	60-240
Single-axis-tracking	Linear Fresnel Reflector	Tubular	5-15	60-300
	Parabolic trough collector (PTC)	Tubular	10-40	60-250
		Tubular	15-45	60-300
	Cylindrical trough collector		10-50	60-300
Two axes tracking	Parabolic dish reflector (PDR)	Point	100-1000	100-500
	Heliostat field collector (HFC)	Point	100-1500	150-2000

2. Materials and method

2.1. Description of the prototype

The experimental device that we studied was designed at the central maintenance workshop of Joseph KI-ZERBO University with a total height of two (02) meters. This chimney is equipped with a collector whose cover has a hyperbolic profile which is placed on a square absorber measuring 2m x 2m painted black on the one hand and made up of hemispherical concentrators on the other hand constituting its base. We used two types of absorbers, namely the plane absorber painted in matt black with a thickness of 0.35mm. It should be noted that the collector of the plane absorber painted in matt black is made of glass surmounted by a chimney whose height varies between 1m to 3 m, and the hemispherical concentrators for the second absorber. Many other materials have been used as absorbers but have not made it possible to reach the temperature level obtained with this material of the plane absorber (more than 87°C

sometimes) which has an average thermal conductivity of the order of 140W/m. K and a density of 2.8 kg/m³ [13]. We used a total of 48 hemispherical concentrators, each 0.28m in diameter, arranged 7x7 to form the absorber during the measurements. Instead of glass, we used a transparent plastic film (polystyrene) to cover the prototype, to create the greenhouse effect and reduce heat exchange with the outside.

Considering the geometry of the device and to make the use of the device easy, our solar chimney has rings to be able to reveal the hyperbolic profile. To cover the roof of the collector we cut the plastic film according to the length differences between the rings of the collector. Covering the roof was made easy thanks to templates that we used to cut the plastic.

To identify the hyperbolic profile, we used the hyperbolic coordinate described by Ousmane et al [14] and which is defined by:

$$\eta = 2xy \tag{1}$$

So, for one meter (1m) of collector radius and 0.125 m of chimney radius, we obtain the following parameters: x=1 and y=0.125. The resulting hyperbolic function taking these parameters into account is written as follows:

$$y = f(x) = \frac{1}{8x} \tag{2}$$

Figure (1) shows a photo of the solar chimney designed for the study.

Figure 1 Photo of the prototype of the solar chimney

2.2. Experimental protocol

The experimental study consisted first of measuring the air temperatures from the collector inlet to the center of the chimney, then those located at different heights in the chimney. These measurements are carried out using 10 type K thermocouples, the 9 of which measure the temperatures and the 10th measures the sunshine received on the site during the day. They have the advantage of having good resistance to radiation but are less satisfactory than type N thermocouples. The thermocouples are connected to a programmable temperature recorder called DATALOGGER (midi LOGGER GL220) connected to different levels of the chimney such as the indicates Figure 2. As for the speed evaluation of the hot air, its flow and the temperature of the air inside the chimney, these are done using an anemometer. All this data is recorded every 5 minutes throughout the day. The different positions of the thermocouples are described as follows:

- Thermocouple 1: measures the temperature at ring 4 located 0.8m from the ground.

- Thermocouple 2: measures the temperature at ring 3 located 0.6m from the ground.
- Thermocouple 3: measures the temperature at ring 2 located 0.4m from the ground.
- Thermocouple 4: measures the temperature at ring 1 located 0.25m from the ground.
- Thermocouple 5: measures the temperature at the collector inlet.
- Thermocouple 6: measures the temperature at the absorber.
- Thermocouple 7: measures the temperature at the chimney outlet.
- Thermocouple 8: measures the temperature at the center of the collector 5 cm from the ground.
- Thermocouple 9: measures the ambient air temperature.
- Thermocouple 10: coupled to the pyranometer to measure sunlight.

The positions of the different thermocouples are shown in Figure 2 below.
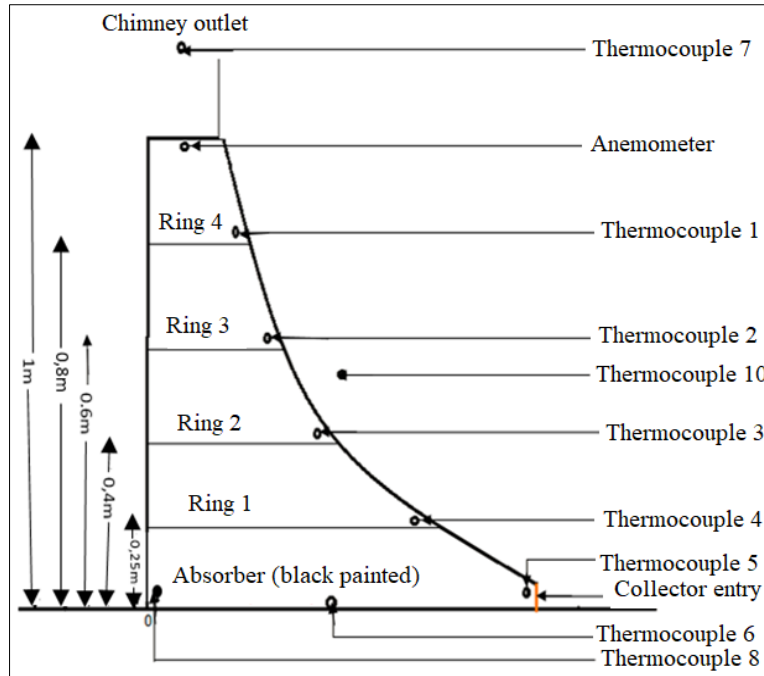
Figure 2 Position of thermocouples along the chimney

The devices used are shown in the figures below:

| **Figure 3** Midi LOGGER GL220 | **Figure 4** Anemometer TESTO 480 | **Figure 5** Pyranometer SR03 |

The experimental data for the days of 10/07/2022 and those of 04/15/2023 were related to the solar tower with a plane absorber. On the other hand, the data from 10/15/2022 and those from 04/10/2023 concerned the solar tower with hemispherical concentrators.

3. Results and discussion

3.1. Experimental study of the solar tower with plane absorber

In this part, we present the variations in temperatures, sunshine and speeds measured during the days of October 7, 2022, and April 15, 2023.

3.1.1. Results and discussions of data for the day of October 7, 2022

Figure 6 below represents the evolution of different temperatures in the solar chimney during the day of October 7, 2022. We note that all the temperature curves have the same shape except that at the entrance to the collector (green curve). The appearance of the temperature at the collector inlet is explained by the fact that thermocouple 5 is placed between two different media. Already from 7 a.m., we observe a rapid increase in the temperature of the absorber (thermocouple 6) which reaches a peak of 98.6°C at 1:08 p.m. It then drops slowly until 5 p.m. This roughly follows the shape of the daily sunshine curve illustrated in Figure 7. After the temperature of the absorber, come respectively the temperatures of ring 1 which is 0.25m from the ground, of ring 2 located at 0.4m with respective peaks observed at 1:13 p.m. of 74.5°C and 67.4°C.

As for the temperatures of rings 3, 4 and that at the chimney outlet, they are also in the same form with some nuances. The ambient temperature and that at the collector inlet change very slowly throughout the day and are very low compared to the rest of the temperatures. Another observation also shows that the temperatures inside the collector drop as we move away from the absorber until the outlet of the chimney. The temperature at the chimney outlet is also higher than that at the collector inlet. This is because the chimney is not thermally insulated, thus contributing to the warming of the temperature at the outlet.
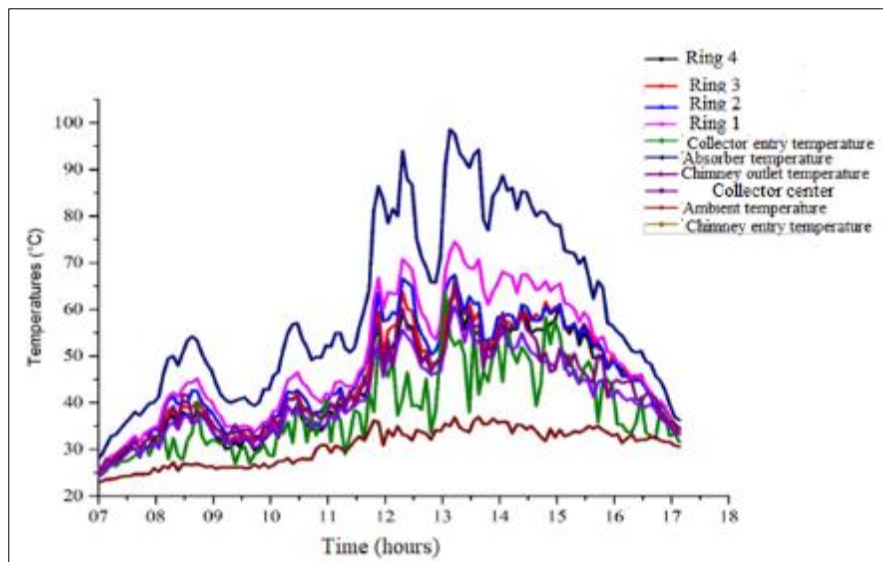

Figure 6 Temperature curves for 07/10/2022

The shape of the sunshine curve for the day of October 7, 2022, is shown in Figure 7 below. We note a growth in this curve from 6 a.m. to 12:18 p.m. with several peaks where it reaches its maximum value of the day: 1204 W/m². Then it gradually decreases until 5 p.m. However, some irregularities were recorded at 9 a.m., 10 a.m., 11 a.m. and between 12 p.m. and 1 p.m. caused by cloudy periods, wind, and dust during the day.
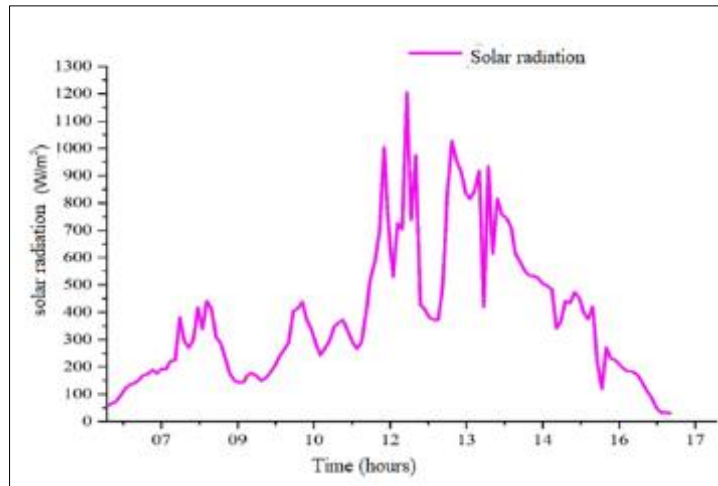
Figure 7 Sunshine curve for 07/10/2022

The appearance in Figure 8 below illustrates the speed curve of the air entering the chimney. By analyzing this curve of the air speed inside the chimney, we observe an increase in the curve first from 7 a.m. to 10:30 a.m., then from 11 a.m. to 12:30 p.m. and finally from 1 p.m. to 1:30 p.m. with slight fluctuations. From 9 a.m. to 10 a.m., then from 1:30 p.m. to 6 p.m., it experiences a drop with a minimum speed of the day which is 0.13 m. s^{-1} due to cloudy periods, wind, and dust. Then it increases gradually until 1:35 p.m. when it reaches its maximum which is 1.81 m. s^{-1}. The observed irregularities are caused by the presence of clouds throughout the day.
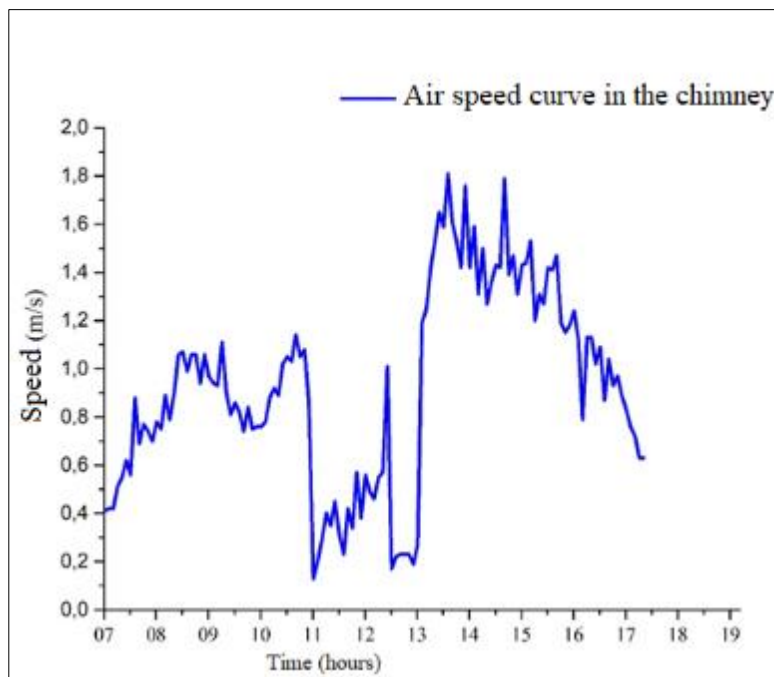

Figure 8 Hot air speed curve in the chimney from 07/10/2022

3.1.2. Results and discussions of data from the day of April 15, 2023

Figure 9 illustrates the temperatures in the solar chimney during the day of April 15, 2023. We notice that the shapes of these temperatures are bell-shaped. From 7 a.m. to 12 p.m., temperatures increase and reach their maximum value, then decrease after 12 p.m. until 5 p.m. The temperature of the absorber increases faster than the others from 7 a.m. and reaches its maximum value of the day which is 97.1°C. It is followed respectively by the temperatures of rings 1, 2, 3, 4, that of the center of the collector, and that of the chimney outlet with some temperature differences. As for the temperature at the collector inlet, it is practically the same as the ambient air temperature from 10 a.m. to 2 p.m. As the

hot air rises towards the chimney, it cools, and this explains the drop in temperature as one rises towards the chimney. We also observe now that the ambient temperature remains low compared to other temperatures.
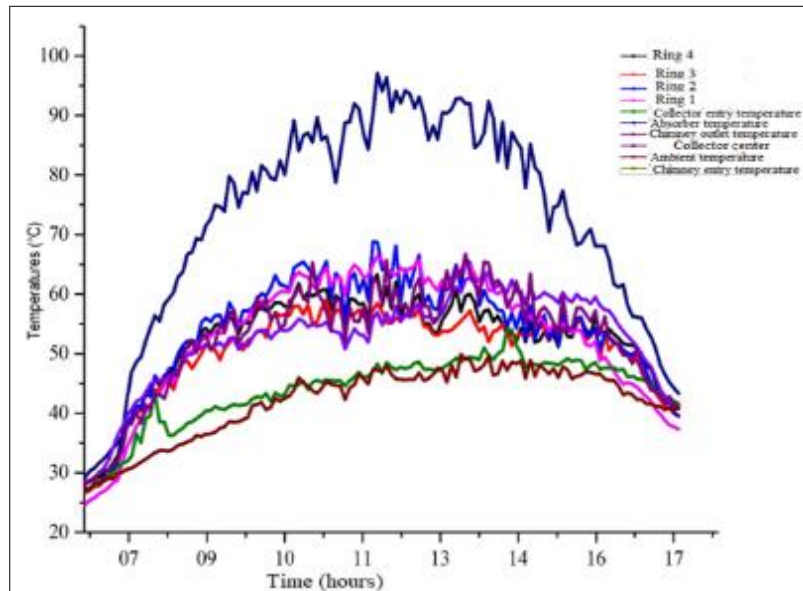

Figure 9 Temperature curves for 04/15/2023

The sunshine data for the day of April 15, 2023, is illustrated in Figure 10 below. This sunshine varies from 29.4 $W.m^{-2}$ to 997.7 $W.m^{-2}$ during the day. We observe that it increases globally from 7 a.m. to 11 a.m. with a maximum value of 997.7 $W.m^{-2}$. From 11 a.m. to 5 p.m., it gradually decreases. The sunlight curve retains its Gaussian (bell-shaped) shape like all radiation curves. The irregularities observed between 2 p.m. and 5 p.m. are caused by cloudy conditions.
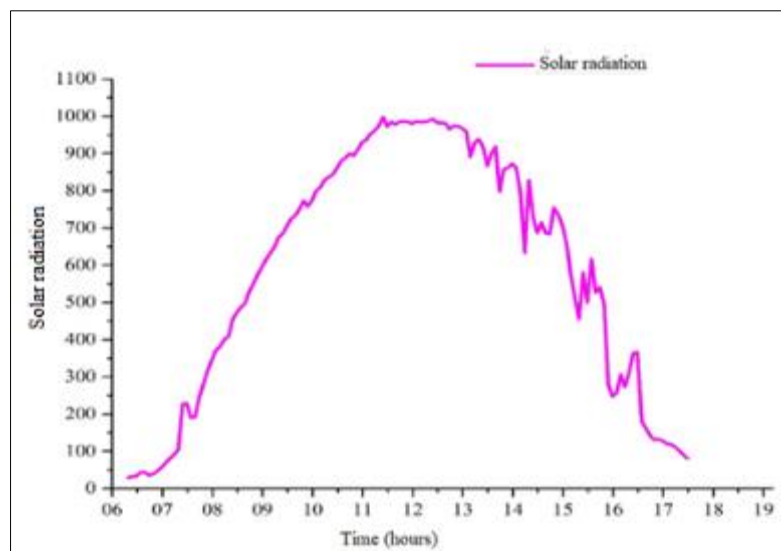

Figure 10 Sunshine curve for 04/15/2023

The appearance of the air speed curve entering the chimney during the day of April 15, 2023, is illustrated in Figure 11 below. By increasing, presents several peaks and reaches a maximum value of 1.06 m. s^{-1} at 10:58 a.m. then decreases until 5 p.m. The appearance has a bell shape with disturbances during the day. These disturbances are caused by wind, cloudy periods.
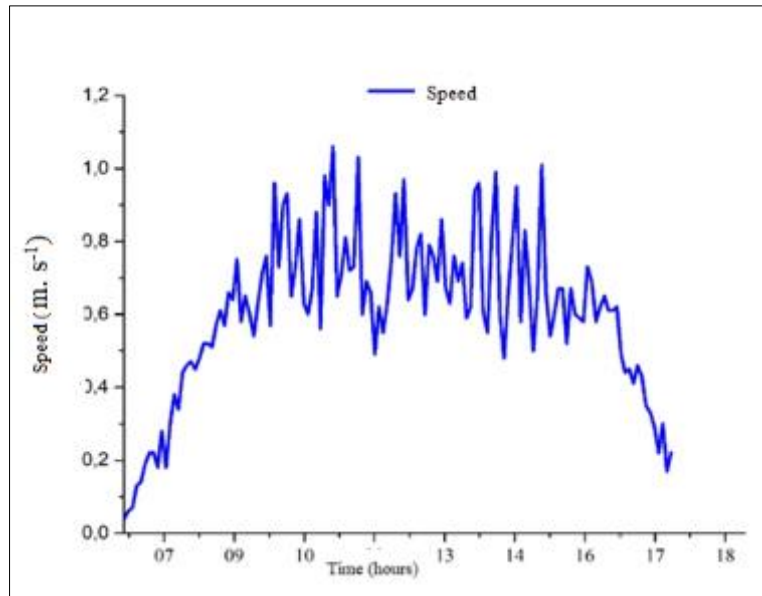
Figure 11 Hot air speed curve in the chimney from 04/15/2023

3.2. Experimental study of the solar tower with hemispherical concentrators

In this part, we present the variations in temperatures, sunshine and speeds measured on October 15, 2022, and April 10, 2023.

3.2.1. Results and discussions of data from the day of October 15, 2022

The evolution of temperatures in the solar chimney is shown in Figure 12 below. These temperature curves are like the previous ones with their bell shape and vary from 22.8°C to 79.8°C. We observe that already from 7 a.m., the temperature of the absorber evolves faster than the others to reach its maximum value of 79.8°C at 12:32 p.m. with maximum sunshine of 1000W.m^{-2}. Then come respectively the temperature curves of the rings 1,2, 3, 4, then the center of the collector, as well as the temperatures at the outlet of the chimney and at the outlet of the collector. They all have the same shape as those of the absorber. In fact, as in the case of the previous measurements, the air heated in the collector becomes light and rises through the chimney effect in the chimney. As it rises, the hot air cools as it exits the chimney.
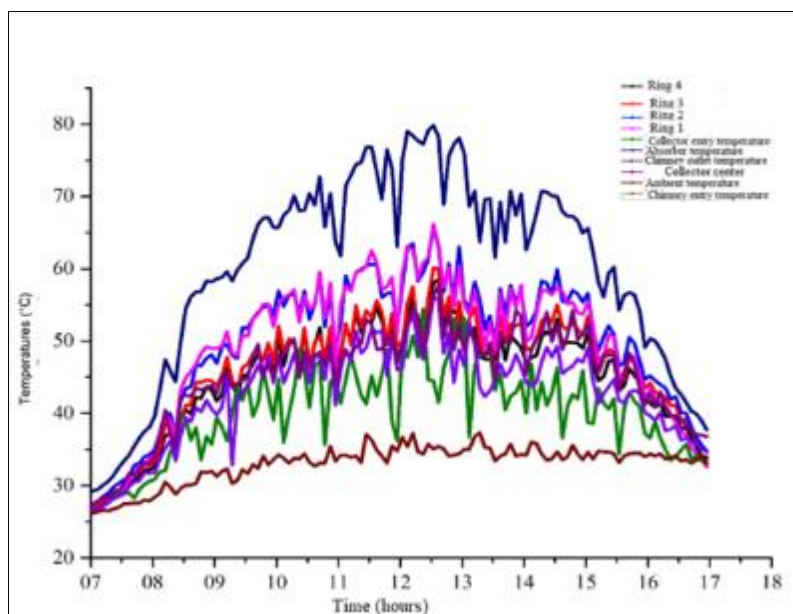

Figure 12 Temperature curves for 10/15/2022

The sunshine data for the day of October 15, 2022, is illustrated in Figure 13 below. These data vary from 2 to 1000 W.m-2 during this day. We observe that the curve increases overall from 7 a.m. to 12 p.m. with a maximum value of 1000 W.m-2 observed around 12 p.m. From 12 p.m. to 5 p.m., it gradually decreases. The sunlight curve retains its Gaussian shape. The irregularities observed throughout the day are caused by cloudy events.
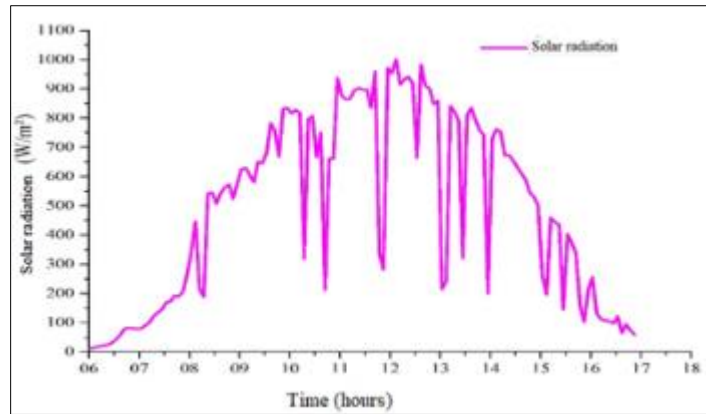

Figure 13 Sunshine curve for 10/15/2022

The appearance of the air speed curve entering the chimney during the day of October 15, 2022, is illustrated in Figure 14 below. It varies from 0.02 m. s^{-1} to its maximum value 2.05 m. s^{-1} at 3:48 p.m. then decreases until 5 p.m. The appearance has a bell shape with disturbances during the day. These disturbances are caused by cloudy periods.
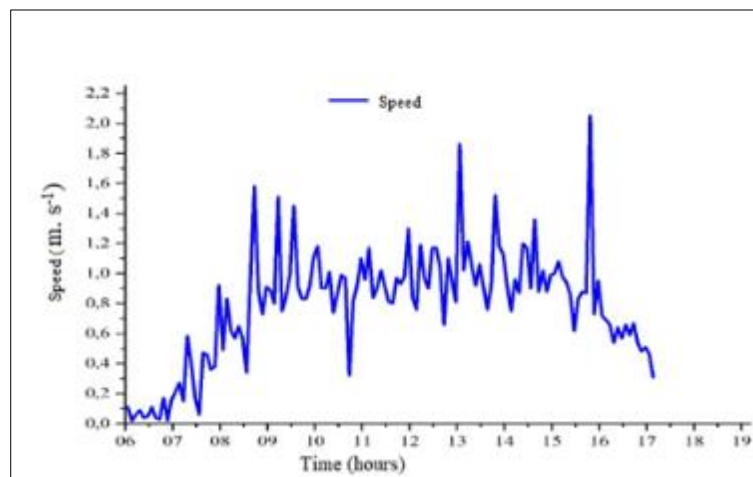

Figure 14 Hot air speed curve in the chimney from 10/15/2022

3.2.2. Results and discussions of data for the day of April 10, 2023

Figure 15 illustrates the temperature variations in the solar chimney during the day of April 10, 2023. We notice that the shapes of these temperatures are bell-shaped. From 7 a.m. to 12 p.m., temperatures increase and reach their maximum value, then decrease after 12 p.m. until 5 p.m. The temperature on the absorber increases faster than the others around 7:30 a.m. and reaches its maximum value for the day: 91.9°C. It is followed respectively by the temperatures of rings 2, 3, 4, 1, that of the center of the collector, and that of the chimney outlet.
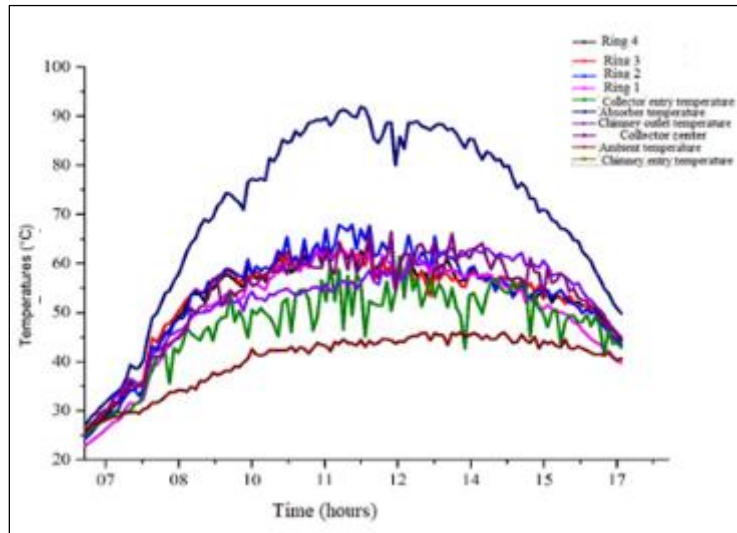
Figure 15 Temperature curves for 04/10/2023

The sunshine data for the day of April 10, 2023, is illustrated in Figure 16 below. This sunshine varies from 17.9 $W.m^{-2}$ to 1007.2 $W.m^{-2}$ during the day. We observe that it increases globally from 7 a.m. to 11 a.m. with a maximum value of 1007.2 $W.m^{-2}$. From 11 a.m. to 5 p.m., it gradually decreases. The sunlight curve retains its bell shape. The irregularities observed between 12 p.m. and 1 p.m. are caused by cloudy periods, dust, and wind.
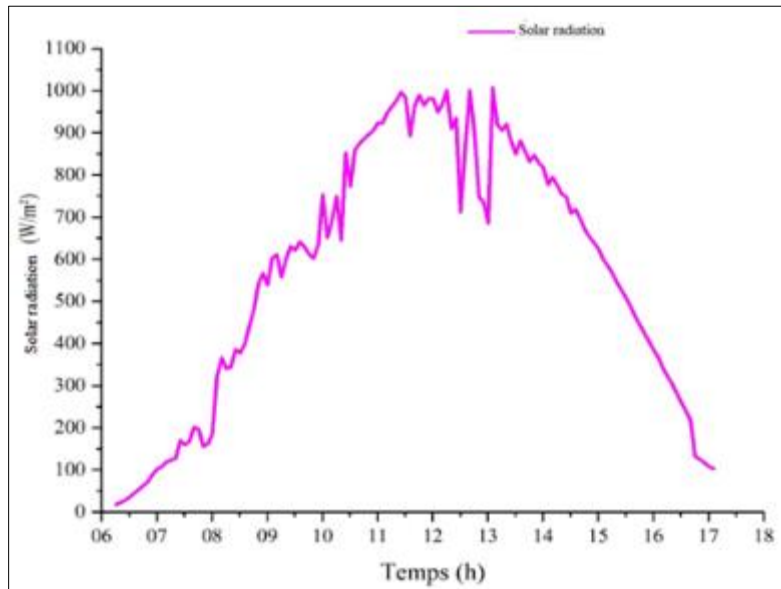

Figure 16 Sunshine curve for 04/10/2023

The shape of the air speed curve entering the chimney during the day of April 10, 2023, is illustrated in Figure 17 below. It varies from 0.04 $m.s^{-1}$ to 1.94 $m.s^{-1}$ and reaches its maximum value 1.94 $m.s^{-1}$ at 2:43 p.m. then decreases until 5 p.m. The appearance has a bell shape with disturbances during the day. These disturbances are caused by cloudy periods.
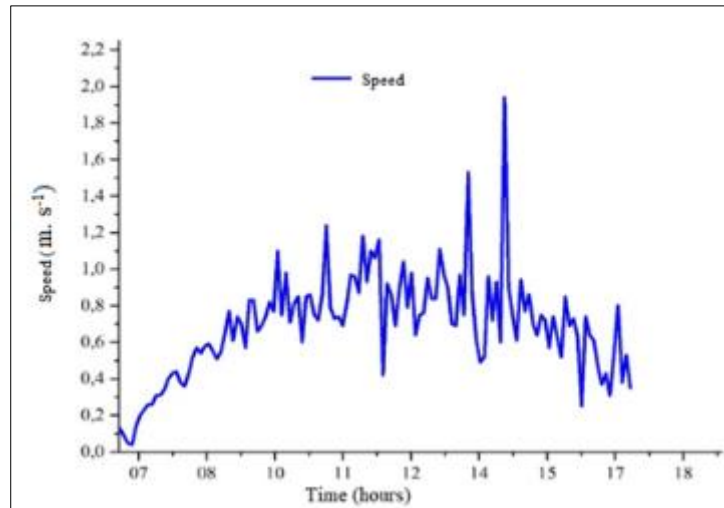
Figure 17 Hot air speed curve in the chimney from 04/10/2023

4. Conclusion

Indeed, during the two measurement periods of October and April we noted that the speed is greater with the hemispherical concentrators than with the flat absorber respectively 1.81 m. s^{-1} during the day of 07/10 /2022 and 1.06 m. s^{-1} during the day of 04/15/2023 for the plane absorber compared to 2.05 m. s^{-1} on 10/15/2022 then 1.94 m. s^{-1} on 04/10/2023 for hemispherical concentrators. This result is confirmed by the work of KY et al [15] based on the results obtained on the experimental study of a solar chimney with a collector made up of hemispherical concentrators. The results obtained allowed them to conclude that hemispherical concentrators could better replace systems with planar absorbers by consequently reducing the usual size of chimney solar collectors. We also show the overall air speed increasing to maximums compared to previous studies.

Based on the temperatures recorded at the different levels of the solar chimney, the results of our experimental study show that the maximum temperature values for the plane absorber are slightly higher than those obtained with the hemispherical concentrators over the same periods of the year. These differences are due to cloud disturbances, wind and dust during the day which have an impact on sunshine, and therefore on temperatures. Thus, with the planar absorber we obtained a maximum experimental value of 98.6°C on 10/07/2022 and 97.1°C on 04/15/2023 compared to 79.8°C on 10/15/2022 and 91.9°C on 04/10/2023 with hemispherical concentrators. Which is contrary to the results based on the speed of the air inside the chimney. However, it should be noted that the maximum absorber temperatures depend on the amount of sunlight on the day. In fact, with the flat absorber we had more sunlight than with the hemispherical concentrators. For example, for the day of 07/10/2022, we had sunshine of 1204 W.m^{-2} corresponding to a maximum temperature of 98.6°C at 1:18 p.m. while for the same period, 15/10/2022, with the hemispherical concentrators the sunshine is 1000 W.m^{-2} corresponding to a maximum temperature of 79.8°C at 12:32 p.m., or approximately one hour less. This shows that with hemispherical concentrators for the same irradiation, we could exceed the maximum temperature values of the plane absorber. We can conclude that hemispherical concentrators can replace the planar absorber. The results of our experimental study made it possible to identify the idea that the solar chimney using hemispherical concentrators can replace that using the planar absorber. The use of plastic as the collector of our device exchanges heat with the outside, thus causing a drop in temperature when it moves towards the outlet of the collector.

Compliance with ethical standards

Acknowledgement

Disclosure of conflict of interest

No conflict of interest to be disclosed.

References

[1]   Kalogirou, S.A. Solar thermal collectors and applications. Progress in Energy and Combustion Science 30 (2004) 231–295.

[2]   TABET, I. Étude, Réalisation et simulation d'un capteur solaire. Thèse. Université des frères Mentouri Constantine faculté des sciences exactes, 2016.

[3]   Zhu, T., Diao Y, Zhao Y, Deng Y. Experimental study on the thermal performance and pressure drop of a solar air collector based on flat micro-heat pipe arrays. Energy Convers Manage 2015; 94 :447–57. https://doi.org/10.1016/j. enconman.2015.01.052.

[4]   Cisse, E.I., Thiam, A., Ndiogou, B.A, Azilinon, D., Sambou, V. Experimental investigation of solar chimney with concentrated collector (SCCC). https://doi.org/10.1016/j.csite.2022.101965

[5]   Chaichan, MT., Abass, KI., Kazem, HA. Dust and pollution deposition impact on a solar chimney performance. International Research Journal of Advanced Engineering and Science, 2018, irjaes.com.

[6]   Ahmed, O.K., Hussein, A.S. New design of solar chimney (case study). Case Studies in Thermal Engineering. Volume 11, March 2018, Pages 105-11. https://doi.org/10.1016/j.csite.2017.12.008.

[7]   Austrian institute of technology. Reliability test of solar collector according to EN12975:2006, Gluatmugl HT; 2008. <http://www.solid.at/images/pdf/

[8]   Platzer WJ. Calculation procedure for collectors with a honeycomb cover of rectangular cross section. Sol Energy 1992;48(6):381–93.

[9]   Harrison SJ, Lin Q, Mesquita LCS. Integral stagnation temperature control for solar collectors. In: SESCI 2004 Conference; 2004.

[10]   Kessentini, H., Castro, j., Capdevila, R., Oliva, A. Development of flat plate collector with plastic transparent insulation and low-cost overheating protection system. Applied Energy 133, 206-223. Elsevier.

[11]   Mandal, D.K., Biswas, N., Manna, N.K., Benim, A.C. Impact of chimney divergence and sloped absorber on energy efficacy of a solar chimney power plant (SCPP). Ain Shams Engineering Journal, Volume 15, Issue 2, February 2024, 102390.

[12]   Li, Y., Liu, S. "Experimental study on thermal performance of a solar chimney combined with PCM," Applied Energy, vol. 114, pp. 172-178, 2014.

[13]   Ousmane, M.; Dianda, B., Kam, S., Konfé, A., KY, T.S. M., Bathiébo, D.J. Experimental Study in Natural Convection. Global Journal of Pure and Applied Sciences Vol. 21, 2015: 155-169.

[14]   Moctar, O., Ky, T.S.M., Konfé, A., Dianda, B., Ouédraogo,S., Bathiébo, D.J. Natural Convection Modeling in a Solar Tower. Indian Journal of Science and Technology. Year: 2021, Volume: 14, Issue: 48, Pages: 3475-3493. 10.17485/IJST/v14i48.1357.

[15]   S. M. T. Ky, S. Ouedraogo, A. Ouedraogo, B. Dianda, M. Ousmane, and D. J. Bathiebo, "Novel convection process: Experimental study of a solar chimney with its collector made of hemispherical concentrators," *Int. J. Eng. Sci. Res. Technol. Nov.*, vol. 7, no. 10, pp. 83–96, 2018, doi: 10.5281/zenodo.1471587.